

ing the remnants of a rhyolitic magma body beneath the resurgent dome since the beginning of unrest in 1980.

References and Notes

1. R. L. Smith and R. A. Bailey, *Mem. Geol. Soc. Am.* **116**, 613 (1968).
2. R. I. Tilling and J. Dvorak, *Nature* **363**, 125 (1993).
3. G. Berrino, *J. Volcanol. Geotherm. Res.* **61**, 293 (1994).
4. D. Dzurlin, K. M. Yamashita, J. W. Kleinman, *Bull. Volcanol.* **56**, 261 (1994).
5. G. De Natale, F. Pingue, P. Allard, A. Zollo, *J. Volcanol. Geotherm. Res.* **48**, 199 (1991).
6. C. Wicks Jr., W. Thatcher, D. Dzurlin, *Science* **282**, 458 (1998).
7. G. Berrino, H. Rymer, G. C. Brown, C. Corrado, *J. Volcanol. Geotherm. Res.* **53**, 11 (1992).
8. R. C. Jachens and C. W. Roberts, *J. Geophys. Res.* **90**, 11210 (1985).
9. A. A. Eggers, *J. Volcanol. Geotherm. Res.* **33**, 201 (1987).
10. Measurements made in the same month may minimize seasonal variations in water table [F. Arnet *et al.*, *Geophys. Res. Lett.* **24**, 2741 (1997)]; sites on low-porosity outcrops (32) or near sea level (30) may minimize water table effects on gravity changes.
11. R. A. Bailey, *Map I-1933* (U.S. Geological Survey, Reston, VA, 1989).
12. ——— and D. P. Hill, *Geosci. Can.* **17**, 175 (1990).
13. J. Langbein *et al.*, *J. Geophys. Res.* **100**, 12487 (1995).
14. B. R. Julian, *Nature* **303**, 323 (1983).
15. C. W. Roberts, R. C. Jachens, R. Morin, *U.S. Geol. Surv. Rep.* **88-50** (1988).
16. The measured gravity differences at each station were processed with a least squares method to obtain one gravity value following the methods described by R. C. Jachens [in *1980 Eruptions of Mount St. Helens, Washington* (U.S. Geological Survey, Reston, VA, 1981), pp. 175–181].
17. J. F. Howle and C. D. Farrar, *U.S. Geol. Surv. Open File Rep.* **96-382** (1996).
18. D. Dzurlin, personal communication.
19. P. Goovaerts, *Geostatistics for Natural Resources Evaluation* (Oxford Univ. Press, New York, 1997).
20. Kriging provides only an incomplete measure of local accuracy and no estimation of joint accuracy when several locations are considered together. Gaussian simulations are designed specifically to provide such measures. Gaussian simulation is the process of drawing alternative, equally probable, joint realizations of a random variable (in our case, the uplift or change in water table depth at a given location) that follows a multivariate Gaussian distribution. The parameters of the Gaussian distribution (mean and variance) are determined by kriging. The random sampling is such that all the realizations fit the existing data exactly. The variance of a set of simulated values provides a measure of local uncertainty for the attribute of interest.
21. S. Rouhani and D. E. Meyers, *Math. Geol.* **22**, 611 (1990).
22. M. L. Sorey, R. E. Lewis, F. H. Olmsted, *U.S. Geol. Surv. Prof. Pap.* **1044-A** (1978).
23. The fact that the station in the eastern caldera with the large residual gravity change experienced an unusually small raw gravity change ($-4 \pm 7 \mu\text{gal}$) compared with neighboring stations in the eastern caldera (with gravity changes of -46 ± 10 , -30 ± 14 , $-42 \pm 11 \mu\text{gal}$) suggests possible measurement errors at this site (see Fig. 3A).
24. B. Efron and R. Tibshirani, *Stat. Sci.* **1**, 54 (1986). The data were randomly resampled with replacement (that is, some stations appear multiple times and others not at all). The resampled data set was inverted for source depth, and the process was repeated several thousand times. Ninety-five percent confidence intervals were determined by ordering the bootstrap results and excluding the smallest and largest 2.5% of the distribution.
25. K. Mogi, *Bull. Earthquake Res. Inst.* **36**, 99 (1958).

26. R. S. Chermichael, Ed., *Handbook of Physical Rock Properties*, vol. III (CRC Press, Boca Raton, FL, 1984).
27. J. B. Walsh and J. R. Rice, *J. Geophys. Res.* **84**, 165 (1979).
28. The estimated volume from gravity is based on data from July 1982 to July 1998. Because leveling was not conducted in 1998, the estimated volume from leveling is based on data from July 1982 to July 1997. Volume change between 1997 and 1998 is thus not accounted for.
29. C. M. Weiland, L. K. Steck, P. B. Dawson, V. A. Korneev, *J. Geophys. Res.* **100**, 20379 (1995).
30. C. McKee, J. Mori, B. Talai, in *Volcanic Hazards: Assessment and Monitoring* (Springer-Verlag, Berlin, 1989), pp. 399–428.
31. B. Talai *et al.*, *Bull. Global Volcanism Network* **22** (no.

- 4) (1997) (available at http://www.volcano.si.edu/gvp/volcano/region05/newbrit/rabaul/var_01.htm 2204).
32. J. B. Rundle and J. H. Whitcomb, *J. Geophys. Res.* **91**, 12675 (1986).
33. F. Barberi, in *Monitoring and Mitigation of Volcano Hazards* (Springer-Verlag, Berlin, 1996), pp. 771–786.
34. C. D. Farrar *et al.*, *Nature* **376**, 675 (1995).
35. M. L. Sorey, C. D. Farrar, G. A. Marshall, J. F. Howle, *J. Geophys. Res.* **100**, 12475 (1995).
36. This work would have not been possible without support and data from several individuals and institutions. In particular, we thank R. Bailey, D. Dzurlin, C. Farrar, D. Hill, J. Langbein, J. Murray, and W. Thatcher.

28 May 1999; accepted 17 August 1999

Impaired Fas Response and Autoimmunity in *Pten*^{+/-} Mice

Antonio Di Cristofano,¹ Paraskevi Kotsi,¹ Yu Feng Peng,³ Carlos Cordon-Cardo,² Keith B. Elkon,³ Pier Paolo Pandolfi^{1*}

Inactivating mutations in the *PTEN* tumor suppressor gene, encoding a phosphatase, occur in three related human autosomal dominant disorders characterized by tumor susceptibility. Here it is shown that *Pten* heterozygous (*Pten*^{+/-}) mutants develop a lethal polyclonal autoimmune disorder with features reminiscent of those observed in Fas-deficient mutants. Fas-mediated apoptosis was impaired in *Pten*^{+/-} mice, and T lymphocytes from these mice show reduced activation-induced cell death and increased proliferation upon activation. Phosphatidylinositol (PI) 3-kinase inhibitors restored Fas responsiveness in *Pten*^{+/-} cells. These results indicate that *Pten* is an essential mediator of the Fas response and a repressor of autoimmunity and thus implicate the PI 3-kinase/Akt pathway in Fas-mediated apoptosis.

The *PTEN* gene encodes a phosphatase homozygously mutated in a high percentage of human tumors (1, 2). Heterozygous inactivation of *PTEN* results in three human dominant disorders: Cowden disease, Bannayan-Zonana syndrome, and Lhermitte-Duclos syndrome (3). Disruption of *Pten* in the mouse results in early embryonic lethality (4). *Pten* heterozygous (*Pten*^{+/-}) mice display hyperplastic-dysplastic features as well as high tumor incidence (4). The complete penetrance of the hyperplastic-dysplastic changes suggests that these features could be due to *Pten* haploinsufficiency. However, the specific biological consequences of *Pten* haploinsufficiency remain unclear as well as whether complete *Pten* inactivation must occur for full neoplastic transformation. A major substrate of PTEN is phosphatidylinositol trisphosphate (PIP-3), a lipid second messenger produced by PI 3-kinase (5). In the absence of *Pten* activity, PIP-3 concentrations

are increased, leading to enhanced phosphorylation and activation of the survival-promoting factor Akt/PKB (6). *Pten*^{-/-} embryonic stem cells and mouse embryonic fibroblasts are protected from some apoptotic stimuli (6), which suggests that *Pten* can inhibit Akt-dependent survival signals induced in response to PI 3-kinase activation. Here, we show that *Pten* haploinsufficiency results in a lethal autoimmune disorder and that Fas-mediated apoptosis is impaired in *Pten*^{+/-} mice.

Almost 100% of *Pten*^{+/-} females (44 of 45, in the C57BL6/129Sv background) developed, between 4 and 5 months of age, a severe lymphadenopathy affecting mainly the submandibular, axillary, and inguinal lymph nodal stations (Fig. 1A). The mice died, most likely of renal failure (see below), before they were 1 year old. Male mutants were more mildly affected, with 33% of the animals (20 of 24) developing less severe lymph node hyperplasia by 8 months of age and surviving up to at least 15 months.

Gross pathological analysis consistently revealed features that are typically observed in autoimmune disorders:

1) The spleen was enlarged and the lymph nodes were markedly hyperplastic (Fig. 1B). Histological examination (7) showed that

¹Department of Human Genetics–Molecular Biology Program, ²Department of Pathology, Memorial Sloan-Kettering Cancer Center, Sloan-Kettering Institute, 1275 York Avenue, New York, NY 10021, USA. ³Hospital for Special Surgery, Cornell University Medical College, New York, NY 10021, USA.

*To whom correspondence should be addressed. E-mail: p-pandolfi@ski.mskcc.org

REPORTS

these organs were characterized by hyperactive features, with partial to total effacement of the normal architecture. Germinal centers displayed hyperplastic changes (Fig. 1, C and D). The expansion of T and B lymphocytes was polyclonal (Fig. 1, E and F), as verified by a flow cytometric analysis (see below).

2) Most other organs were congested, with inflammatory infiltrates. In particular, the lung showed increased thickening of the interstitial alveolar spaces with vascular congestion and, in some instances, complete collapse of the pulmonary lobes (Fig. 1G).

3) The kidneys showed proliferation of mesangial cells and increased extracellular matrix in the glomeruli, accompanied by vacuolization and dilation of proximal tubules, with the presence of proteinaceous material in the lumen. In the most severely affected mice, the glomeruli were segmentally or totally solidified (Fig. 1H), with focal thickening of the capillary walls, a picture of segmental glomerulosclerosis. Similar pathological features are observed in human autoimmune syndromes and in autoimmune-prone mouse strains (8).

To confirm that *Pten*^{+/-} mice suffered from an autoimmune glomerulopathy, we analyzed the kidneys from our mutant animals for the presence of immune complexes deposited in the glomeruli. Immunofluorescence microscopy showed immunocomplex deposition displaying the classical diffuse global granular staining of the capillary walls (Fig. 2A) (9).

As the primary cause for deposition of immune complexes in the kidney is hypergammaglobulinemia with autoantibodies reacting against nuclear antigens [histones, double-stranded DNA, and single-stranded (ss) DNA], we analyzed the immunoglobulin concentrations of tumor-free *Pten*^{+/-} mice and found a marked increase in serum immunoglobulin G (IgG) concentrations relative to wild-type mice (9). This was particularly conspicuous for the females ($P < 0.01$) (Fig. 2B). We next tested the presence in the serum of nuclear antibodies (ANAs) (9). Half the affected females had high titers of ANAs (Fig. 2C). Moreover, almost all the *Pten*^{+/-} female mice analyzed had higher titers of antibodies to ssDNA (anti-ssDNA) (9) relative to wild-type controls ($P < 0.01$) (Fig. 2D). In the *Pten*^{+/-} males the difference with respect to their wild-type counterparts was less striking ($P < 0.05$). Finally, urine analysis of *Pten*^{+/-} mutants revealed the presence of additional features of an autoimmune disorder, such as proteinuria and high leukocyte and hemoglobin concentrations in the most severely affected animals (9).

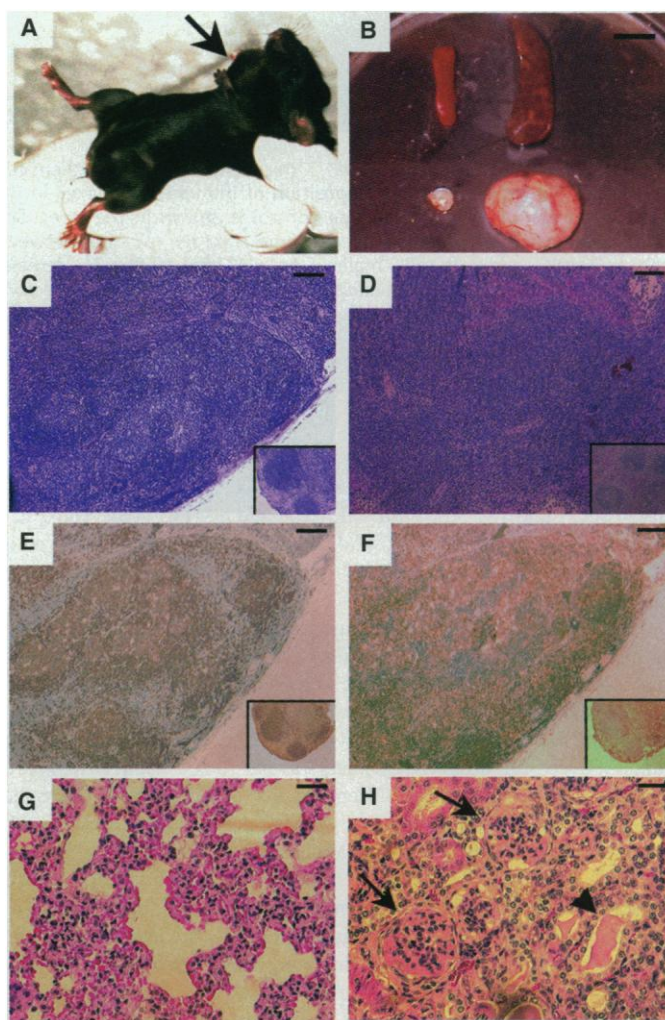
One hallmark of the autoimmune diseases affecting autoimmune-prone mouse strains is the progressive accumulation in the periphery

of activated T and B cells (8, 10). We analyzed spleen and lymph nodes from wild-type and *Pten*^{+/-} mice for the expression of lineage and activation markers (11). The ratio of B and T cells as well as the ratio of CD4⁺ and CD8⁺ T cell subsets was normal in the lymph nodes, confirming the polyclonal nature of the lymphocyte expansion. In contrast, an expansion of the splenic T cell compartment (wild type, 33.3 ± 3.4%; heterozygous, 41.2 ± 0.9%) and an increased CD4⁺ population (CD4⁺/CD8⁺ ratio: wild type, 1.2 ± 0.07; heterozygous, 1.87 ± 0.05) was observed in about 50% of the cases. Contrary to what was found in the *lpr* mutants, *Pten*^{+/-} mice did not show a B220⁺/Thy1⁺ population or a CD4⁻/CD8⁻ T cell subset. Analysis of the T cell activation markers in all cases showed highly increased populations positive

for CD44, CD54, and CD69 (Fig. 3, A and B). Numbers of CD44⁻, B7-2⁻, and CD5⁻ positive B lymphocytes were also doubled. These results show that both T and B cells are activated in *Pten*^{+/-} mice.

The Fas/FasL system plays a crucial role in the maintenance of peripheral tolerance. Fas is up-regulated upon T and B cell activation, leading to the elimination of these cells through Fas-mediated apoptosis (12). Accumulation of Fas^{high} B cells in the spleen of *gld* mice has been explained by the inability of these primed cells to undergo apoptosis (12). We analyzed *Pten*^{+/-} mice for the expression of Fas in peripheral lymphocytes. Strikingly, the number of B cells expressing Fas was increased by a factor of 3 (Fig. 3C). Moreover, the level of expression of Fas on the surface of T and B cells was increased by

Fig. 1. Histopathological analysis of *Pten*^{+/-} mice. (A) Lymph node hyperplasia (arrow) in a 7-month-old *Pten*^{+/-} female mouse. (B) Dissected spleen and lymph node from sex- and age-matched wild-type (left) and *Pten*^{+/-} (right) mice. Scale bar, 1 cm. (C) Photomicrograph of a lymph node from a *Pten*^{+/-} mouse, stained with H&E. Note the hyperreactive germinal centers and the partial effacement of the normal corticomedullary boundaries. Inset: H&E staining of a lymph node from a wild-type mouse, showing well-delineated microanatomical features. (D) Photomicrograph of a spleen from a *Pten*^{+/-} mouse, stained with H&E. Note the hyperreactive white pulp and the partial effacement of the normal spleen histology. Inset: H&E staining of a spleen from a wild-type mouse, showing well-defined white and red pulp. (E) Consecutive section from the lymph node in (C), stained with anti-B220, showing intense staining in the hyperreactive germinal center. Inset: B220 staining of a lymph node from a wild-type mouse. (F) Consecutive section from the lymph node shown in (C) and (E), stained with anti-CD3, showing staining in the areas surrounding the germinal center and part of the medullary zone. Inset: CD3 staining of a lymph node from a wild-type mouse. (G) Photomicrograph of the lung from a *Pten*^{+/-} mouse stained with H&E. Note the increased thickening of the interstitial alveolar spaces. (H) Photomicrograph of the kidney from a *Pten*^{+/-} mouse stained with H&E, showing dilated tubules filled with proteinaceous material (arrowhead) and glomeruli displaying signs of focal proliferation and sclerosis (arrows). Scale bars, 200 μm (C to F); 50 μm (G and H).



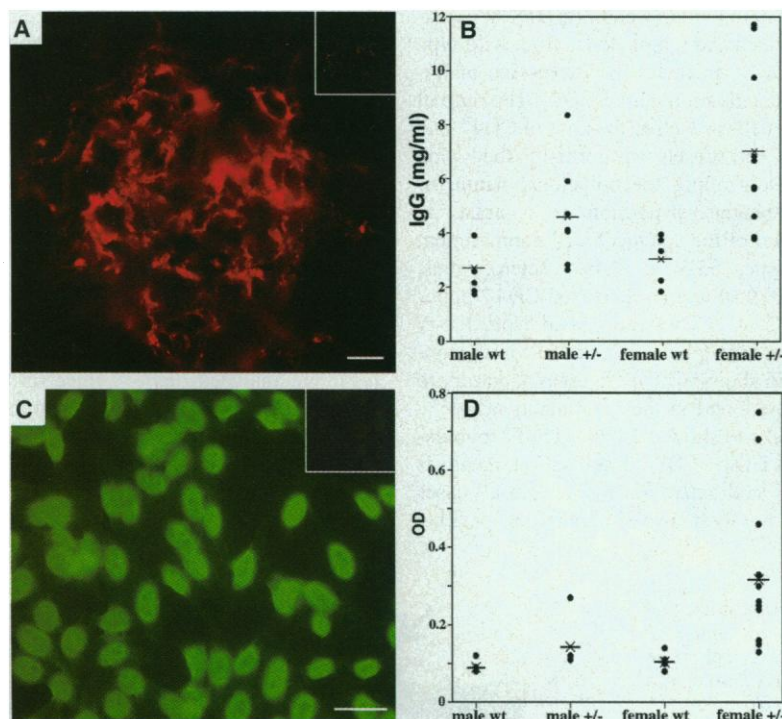


Fig. 2. Autoimmune features in *Pten*^{+/-} mice. **(A)** Immunohistochemical analysis of a kidney from a 9-month-old female, showing deposition of immune complexes in the glomerulus detected by antibody to mouse IgG. A wild-type control is shown in the inset. Scale bar, 1 μ m. **(B)** Serum concentrations of IgG in individual wild-type and *Pten*^{+/-} mice between 6 and 10 months of age ($n = 6$ *Pten*^{+/+} and 8 *Pten*^{+/-} males; 5 *Pten*^{+/+} and 10 *Pten*^{+/-} females). IgG concentrations are expressed in milligrams per milliliter. Means and SD are indicated for each group. **(C)** ANAs in *Pten*^{+/-} mice. Serum was diluted 1:50 and tested by indirect immunofluorescence on HEp-2 cells. A wild-type control is shown in the inset. Scale bar, 1 μ m. **(D)** Titers of anti-ssDNA autoantibodies in the serum of individual wild-type and *Pten*^{+/-} mice ($n = 7$ *Pten*^{+/+} and 6 *Pten*^{+/-} males; 7 *Pten*^{+/+} and 13 *Pten*^{+/-} females). Sera were diluted 1:100 and tested by ELISA. Mean values are indicated for each group.

a factor of 2 to 3 (mean fluorescence intensity: 77 ± 1 and 132.3 ± 9 for wild-type and *Pten*^{+/-} T cells, respectively; 47.4 ± 16 and 122 ± 6 for wild-type and *Pten*^{+/-} B cells, respectively).

The expansion of activated lymphocytes in the presence of a concomitant increase in the expression of Fas cells is suggestive of a defect in Fas-mediated apoptosis. Thus, we analyzed the role of *Pten* in lymphocyte activation, activation-induced cell death (AICD), and Fas-mediated apoptosis. Splenocytes from *Pten*^{+/-} mice proliferated in amounts equal to those in littermate controls in response to treatment with anti-CD3 or lipopolysaccharide (LPS) (13). Concanavalin A (Con A) stimulation, however, resulted in an about 70% increase in proliferation in *Pten*^{+/-} cells (Fig. 4A). Therefore, an enhanced response of *Pten*^{+/-} mature T cells to mitogens might account for at least part of the accumulation of activated cells in the periphery.

To evaluate the sensitivity of *Pten*^{+/-} mature T cells to AICD, we activated CD3e⁺-enriched spleen cells (in the presence of a Fas: Fc chimeric protein, which neutralized mouse Fas ligand) and measured cell death 4 days later (14). *Pten*^{+/-} T cells showed a 50% decrease

in the number of dying cells relative to controls (Fig. 4B). Thus, in the absence of one *Pten* allele, AICD of peripheral T cells is impaired, leading to the expansion of an activated T cell compartment.

We then examined peripheral T and B cells for their sensitivity to apoptosis induced by CD3e and CD95 (Fas) agonistic antibodies (14). Under all experimental conditions, the induction of apoptosis in *Pten*^{+/-}-activated T and B lymphocytes by these stimuli was decreased, even though these cells overexpressed Fas (Fig. 4C). Moreover, we found that *Pten*^{+/-} primary embryonic fibroblasts (PEFs) were also protected from Fas-dependent apoptosis (14) (Fig. 4D). Thus, Fas-mediated signaling is impaired in *Pten*^{+/-} mice and cells.

To investigate the mechanisms underlying the protection from Fas-dependent apoptosis in *Pten*^{+/-} mice, we first analyzed the expression levels of molecules involved in the death-inducing signaling complex (DISC) formation and function and found no difference between wild-type and *Pten*^{+/-} cells (15).

To evaluate whether the protection from Fas-dependent apoptosis could be attributed

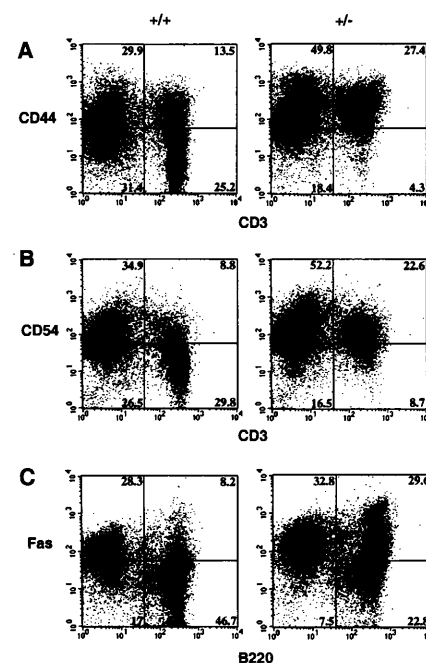


Fig. 3. Expression of activation markers on T and B lymphocytes from gender- and age-matched wild-type and *Pten*^{+/-} mice. Spleen cells were double-stained as indicated (**A** to **C**) and analyzed by flow cytometry. Percentages of analyzed cells are shown in each quadrant.

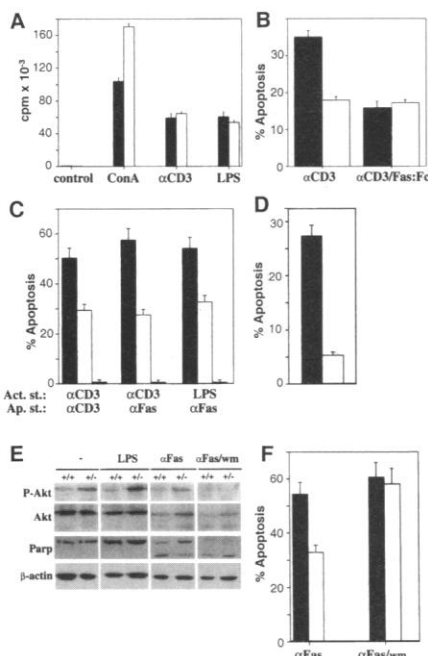
to a PI 3-kinase/Akt-dependent pathway, we analyzed the phosphorylation status of Akt in wild-type and *Pten*^{+/-} splenocytes (15). Akt was hyperphosphorylated in both freshly isolated and LPS-activated *Pten*^{+/-} splenocytes (Fig. 4E). Similar results were obtained in splenocytes activated with Con A.

Akt is degraded early, along with Parp, upon the activation of the caspase proteolytic cascade (16). We therefore analyzed the amount of Akt and Parp after anti-Fas treatment and found that the caspase-dependent degradation of these proteins was severely impaired in *Pten*^{+/-} cells. These differences were abrogated by wortmannin (Fig. 4E). Moreover, pretreatment of the cells with wortmannin completely restored the sensitivity of *Pten*^{+/-} cells to Fas (Fig. 4F). These data indicate a pivotal role for *Pten* haploinsufficiency-dependent Akt activation in the protection from Fas-induced apoptosis observed in *Pten*^{+/-} cells.

In summary, our findings lead to two major conclusions: (i) *Pten* function is crucial for Fas-mediated elimination of activated lymphocytes, including self reactive cells in the periphery, and (ii) inactivation of one *Pten* allele increases the survival and proliferation of certain cell types. In principle, this could lead to the accumulation of further mutations, including loss of heterozygosity at the *Pten* locus, which would ultimately result in full neoplastic transformation. Thus, *Pten* may exert its tumor

REPORTS

Fig. 4. Increased response to Con A and reduced Fas-dependent apoptosis in *Pten*^{+/-} mice. Error bars represent SD. (A) [³H]Thymidine incorporation of activated wild-type (black bar) and *Pten*^{+/-} (white bar) splenocytes. Cells were stimulated for 72 hours as indicated; [³H]thymidine was added for the last 16 hours. (B) Reduced AICD in *Pten*^{+/-} T lymphocytes. CD3⁺-enriched spleen cells were activated with plate-bound anti-CD3 ϵ with or without Fas:Fc chimeric protein (10 μ g/ml), and cell death was determined at day 4 by trypan blue exclusion and in situ TUNEL assay. Wild type, black bar; *Pten*^{+/-}, white bar. (C) Impaired anti-CD3 ϵ and anti-CD95/Fas-induced apoptosis in activated T and B cells. Total spleen lymphocytes or CD3⁺-enriched cells were stimulated for 4 days with cross-linked anti-CD3 ϵ or for 3 days with LPS. Live cells were purified and plated in the presence of plate-bound anti-CD3 ϵ or anti-CD95/Fas for 24 to 48 hours. Cell death was determined as in (B) and is expressed as specific apoptosis (spontaneous apoptosis from untreated control samples has been subtracted from the corresponding treated samples). Wild type, black bar; *Pten*^{+/-}, white bar; *lpr*, gray bar. Act. st., activation stimulus; Ap. st., apoptotic stimulus. (D) Impaired anti-CD95/Fas-induced apoptosis in *Pten*^{+/-} PEFs. Fibroblasts were treated with anti-CD95/Fas for 18 hours. Cell death was determined by Annexin V staining and is expressed as specific apoptosis. Wild type, black bar; *Pten*^{+/-}, white bar. (E) Protein immunoblot analysis of protein extracts from freshly isolated (-), LPS-activated (LPS), and anti-Fas-stimulated splenocytes in the absence (α Fas) or presence (α Fas/wm) of wortmannin. β -Actin was used to show equal loading. (F) Wortmannin restores anti-CD95/Fas-induced apoptosis in activated B cells. Total spleen lymphocytes were stimulated for 3 days with LPS. Live cells were purified and plated in the presence of plate-bound anti-CD95/Fas for 24 hours. Cell death was determined as in (B). Wild type, black bar; *Pten*^{+/-}, white bar. Error bars represent SD.



suppressor function by facilitating programmed cell death upon DNA damage or neoplastic transformation. These data are consistent with the fact that *Pten*^{+/-} mutants develop T and B cell lymphomas (4), which originate from cells that are particularly sensitive to the action of Fas (17), and provide physiological evidence suggesting that PTEN negatively regulates a PI 3-kinase/Akt-dependent pathway for the suppression of Fas induced apoptosis.

References and Notes

- Li et al., *Science* **275**, 1943 (1997); P. A. Steck et al., *Nature Genet.* **15**, 356 (1997).
- B. K. Rasheed et al., *Cancer Res.* **57**, 4187 (1997); H. Tashiro et al., *ibid.*, p. 3935; P. Cairns et al., *ibid.*, p. 4997; E. Rhei et al., *ibid.*, p. 3657.
- D. Liaw et al., *Nature Genet.* **16**, 64 (1997); D. J. Marsh et al., *J. Med. Genet.* **35**, 881 (1998); D. J. Marsh et al., *Hum. Mol. Genet.* **7**, 507 (1998).
- A. Di Cristofano, B. Pesce, C. Cordon-Cardo, P. P. Pandolfi, *Nature Genet.* **19**, 348 (1998); A. Suzuki et al., *Curr. Biol.* **8**, 1169 (1998); K. Podsypanina et al., *Proc. Natl. Acad. Sci. U.S.A.* **96**, 1563 (1999).
- T. Maehama and J. E. Dixon, *J. Biol. Chem.* **273**, 13375 (1998).
- M. P. Myers et al., *Proc. Natl. Acad. Sci. U.S.A.* **95**, 13513 (1998); J. Li et al., *Cancer Res.* **58**, 5667 (1998); P. L. Dahia et al., *Hum. Mol. Genet.* **8**, 185 (1999); V. Stambolic et al., *Cell* **95**, 29 (1998).
- Tissue samples were fixed in 10% buffered formalin. Sections (5 μ m) were stained with hematoxylin and eosin (H&E). Immunophenotyping was done with an avidin-biotin immunoperoxidase technique. Anti-CD3 (purified rabbit serum, 1:1000; Dako), and

anti-B220 (rat monoclonal, 1:1000; PharMingen) were incubated overnight at 4°C. Samples were later incubated with biotinylated secondary antibodies (Vector Labs) for 30 min (goat antibody to rabbit IgG, 1:100; rabbit antibody to rat IgG, 1:100), and then with avidin-biotin peroxidase (1:25 dilution, Vector Labs) for 30 min. Diaminobenzidine was used as the chromogen and hematoxylin was used as the counterstain.

- Mice harboring mutations in the Fas (*lpr*) or Fas ligand (*gld*) genes develop splenomegaly and lymphadenopathy due to massive lymphocyte accumulation and autoimmune nephritis in some genetic backgrounds [R. Watanabe-Fukunaga et al., *Nature* **356**, 314 (1992); T. Takahashi et al., *Cell* **76**, 969 (1994)]. Human autoimmune lymphoproliferative disorder is also characterized by mutations in these genes [M. S. Lim et al., *Am. J. Pathol.* **153**, 1541 (1998)]. NZB/W mice, considered a model for human systemic lupus erythematosus, develop lymphadenopathy and lethal glomerulonephritis with earlier onset in females [L. Morel and E. K. Wakeland, *Curr. Opin. Immunol.* **10**, 718 (1998)]. Mice with a disrupted interleukin-2 (IL-2)/IL-2 receptor system show splenomegaly and lymphadenopathy, autoantibody production, and impaired Fas-dependent apoptosis [D. M. Willerford et al., *Immunity* **3**, 521 (1995); B. Sadlack et al., *Cell* **75**, 253 (1993)].
- Frozen kidney sections from wild-type and *Pten*^{+/-} mice were fixed with cold acetone and blocked in phosphate-buffered saline (PBS) with 0.1% Triton X-100 and 10% goat serum at room temperature. The samples were then stained with Texas Red-conjugated goat antibody to mouse IgG (Jackson ImmunoResearch) for 1 hour at room temperature. ANAs were detected by indirect immunofluorescence on Hep-2 cells. For these assays, sera were diluted 1:50. Total IgG and anti-ssDNA autoantibodies were quantified by enzyme-linked immunosorbent assay (ELISA) as described [D. Mevorach, J. L. Zhou, X. Song, K. B. Elkon, *J. Exp. Med.* **188**, 387 (1998)], with a 1:100 dilution of the sera. All

the data were analyzed by Student's *t* test. Urine samples were spotted on Chemstrip Test Dipstick (Boehringer); values of 2+ or more were considered as positive.

- L. Reininger et al., *J. Exp. Med.* **184**, 853 (1996).
- Single-cell suspensions of spleen and lymph nodes were depleted of mature red blood cells by hypotonic lysis and were stained with the following conjugated antibodies: anti-CD3 ϵ , anti-B220, anti-Thy1, anti-CD4, anti-CD8a (lineage markers); anti-CD5, anti-CD95, anti-CD54, anti-CD69, anti-CD44, anti-B7-2 (activation markers). All antibodies were from PharMingen. Flow cytometry was done with a FAC-Scan (Becton Dickinson) and the data were analyzed with CELLQuest software (Becton Dickinson).
- J. S. Levine and J. S. Koh, *Semin. Nephrol.* **19**, 34 (1999); L. Van Parijs and A. K. Abbas, *Curr. Opin. Immunol.* **8**, 355 (1996); K. B. Elkon and A. Marshak-Rothstein, *ibid.*, p. 852; J. P. Weintraub, R. A. Eisenberg, P. L. Cohen, *J. Immunol.* **159**, 4117 (1997).
- Splenocytes (2×10^5) were cultured in 96-well plates in 100 μ l of RPMI 1640 medium with 10% fetal calf serum. Cells were stimulated by the addition of LPS (100 μ g/ml, Sigma) or Con A (3 μ g/ml, Sigma). For stimulation with plate-bound anti-CD3 ϵ (PharMingen), plates were coated overnight at 4°C with antibody in PBS (10 μ g/ml), then washed twice with PBS/1% bovine serum albumin. After 48 hours, [³H]thymidine (1 μ Ci per well, Amersham) was added, and the cells were harvested 16 hours later for analysis. Addition of recombinant mouse IL-2 (1 to 100 U/ml, Boehringer) to the Con A-stimulated cells did not alter the results.
- CD3⁺ splenocytes enriched by negative selection columns (R&D Systems) were cultured at 2×10^6 cells per milliliter on plate-bound anti-CD3 ϵ with or without Fas:Fc chimeric protein (10 μ g/ml, PharMingen) [T. Suda and S. Nagata, *J. Exp. Med.* **179**, 873 (1994)]. At day 4 of activation, cells were analyzed by trypan blue exclusion count and by in situ terminal deoxynucleotidyl transferase-mediated deoxyuridine triphosphate niche end labeling (TUNEL, Boehringer) on Cytospin slides. At least 500 cells were scored for each experimental point using a fluorescence microscope. For apoptosis induced by CD3 ϵ and CD95 (Fas) agonistic antibodies, splenocytes or CD3⁺ cells were activated as above or in the presence of LPS (100 μ g/ml). At day 3 (LPS) or day 4 (CD3), viable cells were purified by Ficoll (Pharmacia) gradient centrifugation and plated on cross-linked anti-CD3 ϵ (10 μ g/ml) or anti-CD95 (1 to 10 μ g/ml) (Jo2, PharMingen). Apoptosis was determined after 24 or 48 hours by in situ TUNEL. In some cases cells were incubated 30 min at 37°C in the presence of 1 μ M wortmannin (Sigma) before anti-CD95 treatment. PEFs were derived from 14.5-day-old embryos. Anti-CD95 was added at 100 ng/ml in the presence of actinomycin D (0.25 μ g/ml). Cell death was determined 18 hours later by trypan blue exclusion and Annexin V staining (PharMingen).
- Splenocytes were activated with Con A (3 μ g/ml) for 3 days. The expression patterns of *FasL*, *Flip*, and *Fadd* were compared by semiquantitative reverse transcription polymerase chain reaction (PCR). The amount of the cDNA reaction mixture used for PCR amplification was normalized by amplification of the *Hprt* transcript. Primer sequences and amplification conditions are available upon request. Protein immunoblot analysis was performed with anti-Fadd, anti-Flip, and anti-Caspase 8 (Santa Cruz); Anti-PhosphoAkt (Ser⁴⁷³) and anti-Akt (New England Biolabs); anti-PARP (PharMingen); and anti- β -actin (Sigma).
- C. Widmann, S. Gibson, G. L. Johnson, *J. Biol. Chem.* **273**, 7141 (1998); Y. A. Lazebnik et al., *Nature* **371**, 346 (1994).
- J. M. Penninger and G. Kroemer, *Adv. Immunol.* **68**, 51 (1998); M. J. Lenardo, *Semin. Immunol.* **9**, 1 (1997).
- We thank J. L. Zhou for help with the ELISA, M. Jiao for preparation of pathological samples, and M. De Acetis for help with protein immunoblots and mice. P.P.P. is a Scholar of the Leukemia Society of America. Supported by National Cancer Institute grants CA-08748 and CA-82328 and the I. T. Hirsch/M. Weill-Caulier Foundation (P.P.P.), and by NIH grant AR45482 and the Systemic Lupus Erythematosus Foundation, New York (K.B.E.).

24 June 1999; accepted 26 August 1999

LINKED CITATIONS

- Page 1 of 1 -



You have printed the following article:

Impaired Fas Response and Autoimmunity in Pten ⁺/₋ Mice

Antonio Di Cristofano; Paraskevi Kotsi; Yu Feng Peng; Carlos Cordon-Cardo; Keith B. Elkon; Pier Paolo Pandolfi

Science, New Series, Vol. 285, No. 5436. (Sep. 24, 1999), pp. 2122-2125.

Stable URL:

<http://links.jstor.org/sici?sici=0036-8075%2819990924%293%3A285%3A5436%3C2122%3AIFRAAI%3E2.0.CO%3B2-J>

This article references the following linked citations:

References and Notes

¹ **PTEN, a Putative Protein Tyrosine Phosphatase Gene Mutated in Human Brain, Breast, and Prostate Cancer**

Jing Li; Clifford Yen; Danny Liaw; Katrina Podsypanina; Shikha Bose; Steven I. Wang; Janusz Puc; Christa Miliareisis; Linda Rodgers; Richard McCombie; Sandra H. Bigner; Beppino C. Giovannella; Michael Ittmann; Ben Tycko; Hanina Hibshoosh; Michael H. Wigler; Ramon Parsons

Science, New Series, Vol. 275, No. 5308. (Mar. 28, 1997), pp. 1943-1947.

Stable URL:

<http://links.jstor.org/sici?sici=0036-8075%2819970328%293%3A275%3A5308%3C1943%3APAPPTP%3E2.0.CO%3B2-D>

⁴ **Mutation of Pten/Mmac1 in Mice Causes Neoplasia in Multiple Organ Systems**

Katrina Podsypanina; Lora Hedrick Ellenson; Adriana Nemes; Jianguo Gu; Masahito Tamura; Kenneth M. Yamada; Carlos Cordon-Cardo; Giorgio Catoretti; Peter E. Fisher; Ramon Parsons

Proceedings of the National Academy of Sciences of the United States of America, Vol. 96, No. 4. (Feb. 16, 1999), pp. 1563-1568.

Stable URL:

<http://links.jstor.org/sici?sici=0027-8424%2819990216%2996%3A4%3C1563%3AMOPIMC%3E2.0.CO%3B2-T>

⁶ **The Lipid Phosphatase Activity of PTEN is Critical for Its Tumor Suppressor Function**

Michael P. Myers; Ian Pass; Ian H. Batty; Jeroen Van Der Kaay; Javor P. Stolarov; Brian A. Hemmings; Michael H. Wigler; C. Peter Downes; Nicholas K. Tonks

Proceedings of the National Academy of Sciences of the United States of America, Vol. 95, No. 23. (Nov. 10, 1998), pp. 13513-13518.

Stable URL:

<http://links.jstor.org/sici?sici=0027-8424%2819981110%2995%3A23%3C13513%3ATLPAOP%3E2.0.CO%3B2-Z>

NOTE: The reference numbering from the original has been maintained in this citation list.